Journal of Alloys and Compounds 504 (2010) 579–584

Contents lists available at ScienceDirect

Journal of Alloys and Compounds

journal homepage: www.elsevier.com/locate/jallcom

Synthesis, crystal structure and photoluminescence of Eu-α-SiAlON

Kousuke Shioi [a,*], Naoto Hirosaki [b], Rong-Jun Xie [b], Takashi Takeda [b], Yuan Qiang Li [b]

[a] SHOWA DENKO K.K., R and D Center, 1-1-1 Ohnodai, Midori, Chiba 267-0056, Japan
[b] National Institute for Materials Science, Tsukuba, Ibaraki 305-0044, Japan

ARTICLE INFO

Article history:
Received 29 March 2010
Received in revised form 23 May 2010
Accepted 29 May 2010
Available online 11 June 2010

Keywords:
SiAlON
Nitride
Synthesis
Structure
Luminescence

ABSTRACT

Eu-α-SiAlON ($Eu_{m/2}Si_{12-m-n}Al_{m+n}O_nN_{16-n}$) was synthesized with nominal compositions having small m and n values, by firing the powder mixture of $Eu_2Si_5N_8$, α-Si_3N_4, AlN, and Al_2O_3 at 1900 °C for 6 h under 1 MPa nitrogen atmosphere. The ratio of the oxidation state of Eu^{2+}/Eu^{3+} was estimated from the X-ray absorption fine structure (XAFS) measurement. The observed X-ray absorption near edge spectrum (XANES) showed that the Eu ion in Eu-α-SiAlON was mainly in divalent state but also coexisted with a small amount of Eu in the trivalent state. The crystal structure of Eu-α-SiAlON was refined by the Rietveld analysis of the X-ray powder diffraction patterns. The lattice constants of the samples increased with increasing m and n values. The excitation band of Eu-α-SiAlON ranged from the ultraviolet to the visible light region and a broad emission band centered at about 590 nm were observed. The emission intensity decreased significantly with increasing the ratio of trivalent Eu ion, suggesting that the trivalent Eu could be one of the luminescent killer centers.

1. Introduction

White light-emitting diodes (white-LEDs) are becoming next generation solid-state lighting systems due to their low power consumption, high efficiency, long lifetime, and compactness, as well as lack of mercury. In the past ten years, novel rare-earth doped (oxy)nitride phosphors have been drawn considerable attention as their unique structures, high chemical and thermal stability, promising luminescence properties that enable them to be used in white-LEDs. Red $M_2Si_5N_8:Eu^{2+}$ (M = Ca, Sr, and Ba) [1,2], $CaAlSiN_3:Eu^{2+}$ [3,4], and $Sr_xCa_{1-x}AlSiN_3:Eu^{3+}$ [5], orange-red $SrSiAl_4N_7:Eu^{2+}$ [6], yellow Ca-α-SiAlON:Eu^{2+} [7–10], green β-SiAlON:Eu^{2+} [11], $Sr_3Si_{13}Al_3O_2N_{21}:Eu^{2+}$ [12], and $Sr_5Si_{21-x}Al_{5+x}O_{2+x}N_{35-x}:Eu^{2+}$ ($x \approx 0$) [13], and yellow Ce-melilite [14] are just few typical such examples. Among these (oxy)nitride luminescence materials, Eu^{2+}-doped α-SiAlON has a strong absorption in the range of UV-470 nm and exhibits a broad yellow emission [8], which has been proved to be a good conversion phosphor for white light-emitting diodes when combined with a blue LED chip [15].

α-SiAlON ceramics have been widely studied as structural materials because of their excellent mechanical properties and high thermal stability. It has an overall composition given by the formula:

$$M_{m/v}Si_{12-m-n}Al_{m+n}O_nN_{16-n} \quad (1)$$

where M is the modifying cation such as Li, Mg, Ca, Y and rare earth (excluding La, Ce, Pr and Eu), and v is the valence of the cation M. The crystal structure of α-SiAlON can be derived from α-Si_3N_4 by partial cross-substitution of Si^{4+} for Al^{3+} and N^{3-} for O^{2-} which meanwhile is stabilized by trapping cations M into the interstices of the (Si, Al)–$(O, N)_4$ network [16]. Generally, Eu^{2+} ion alone cannot stabilize the α-SiAlON structure due to its large ionic size, but it is possible if Eu^{2+} is co-doped with yttrium or other rare earth ions. Shen et al. addressed that the reaction products from the powder mixture with the composition of Eu-α-SiAlON was the mixture of (α + β)-SiAlON and the unidentified phase [17]. Similar observations were also reported by Jiang et al. [18]. A common feature of these reports is that the composition of Eu single-doped α-SiAlON has large m and n values. Recently, we reported the synthesis, crystal structure, and photoluminescence of Sr containing α-SiAlON ($Sr_{m/2}Si_{12-m-n}Al_{m+n}O_nN_{16-n}:Eu^{2+}$) phosphors having the compositions with small m and n values [19]. It clearly indicates that Sr-α-SiAlON can be formed as the major phase in compositions with small m and n values (m = 0.70–0.80 and n = 0–0.05) [19]. In the present investigation, the synthesis of Eu-α-SiAlON with small m and n in the nominal compositions was attempted according to the routine of Sr-α-SiAlON, due to the similarity of the ionic size between Eu^{2+} and Sr^{2+}. The oxidation state of Eu was estimated from XANES spectra, and then the crystal structure of Eu-α-SiAlON was analyzed by the Rietveld refinement. Finally, the luminescent

* Corresponding author. Tel.: +81 29 851 3354x8865; fax: +81 29 851 3613.
E-mail address: SHIOI.Kousuke@nims.go.jp (K. Shioi).

0925-8388/$ – see front matter © 2010 Elsevier B.V. All rights reserved.
doi:10.1016/j.jallcom.2010.05.164

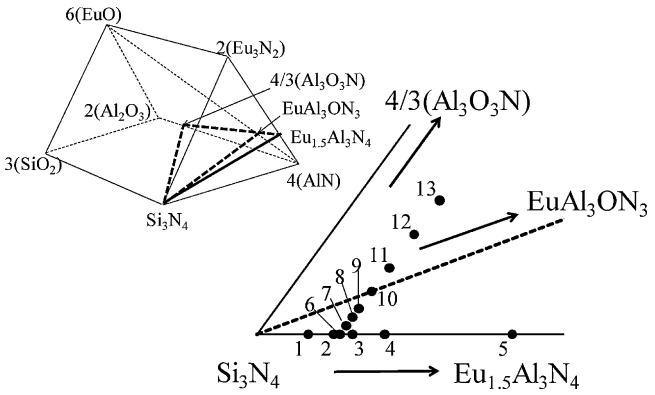

Fig. 1. Schematic illustration of the Eu-α-SiAlON plane with the composition numbers in Table 1.

properties of Eu-α-SiAlON were discussed in detail in comparison with Sr-α-SiAlON.

2. Experimental

Eu-α-SiAlON samples were prepared from α-Si_3N_4 (SN-E10, Ube Industries Ltd., Japan), AlN (Type F, Tokuyama Co. Ltd., Japan) and Al_2O_3 (TM-DAR, Taimei Chemicals Co. Ltd., Japan), and $Eu_2Si_5N_8$, which was pre-synthesized and used as the Eu^{2+} source to investigate small n compositions with an aim to eliminate the influence of the oxidation of raw materials in air, because $Eu_2Si_5N_8$ is very stable against oxidation compared with metallic Eu or EuN. Al_2O_3 was employed to control the oxygen content (n value). $Eu_2Si_5N_8$ was synthesized by the carbothermal reduction and nitridation method [20] from the mixture of Eu_2O_3 (Shin-Etsu Chemical Co. Ltd., Japan), α-Si_3N_4 (SN-E10, Ube Industries Ltd., Japan) and graphite (Type V598, SGL carbon group, Germany). The powder mixture was then loaded into the graphite crucibles and fired under high-purity nitrogen in a horizontal tube furnace at 1600 °C for 4 h. X-ray powder diffraction (XRD) pattern of the obtained sample was in good agreement with a reference of $Eu_2Si_5N_8$ (ICSD #91001).

The nominal chemical compositions of samples were indicated in Fig. 1 and listed in Table 1 in detail. Eu_3N_2, $EuAl_3ON_3$, and $Eu_{1.5}Al_3N_4$ were employed as virtual compounds to show the Eu^{2+} containing phase diagram in Fig. 1. It is worth noting that these virtual compounds are only meaningful for representing their relationships in the phase diagram.

The powder mixtures were ground in the Si_3N_4 mortar and pestle. The mixed powders were loaded into h-BN crucibles and then fired in a graphite resistance furnace at 1900 °C for 6 h under 1 MPa nitrogen atmosphere. The phase products of the synthesized powders were identified by XRD, operating at 40 kV and 40 mA and using CuKα radiation (Ultima III, Rigaku, Japan). A step size of 0.02° 2θ was used with a scan speed of 2°/min for the phase identification. XRD data for Rietveld refinements were recorded at 0.01° intervals counting for 4 s per step. The crystal structures were refined by the Rietveld method using the computer program RIETAN-FP [21], and then visualized by using the software package VESTA [22].

The XAFS spectra of $Eu\text{-}L_{III}$ were collected in the transmission mode at BL14B2 in SPring-8. The incident X-ray was obtained using a double-crystal Si (1 1 1) monochromator. The intensities of the incident and transmitted X-rays were detected by ion chambers. The XAFS spectra of $Eu_2Si_5N_8$ and Eu_2O_3 were also observed as the references. The ratio of Eu^{3+}/Eu^{2+} of selected samples was estimated from XANES spectra using ATHENA program.

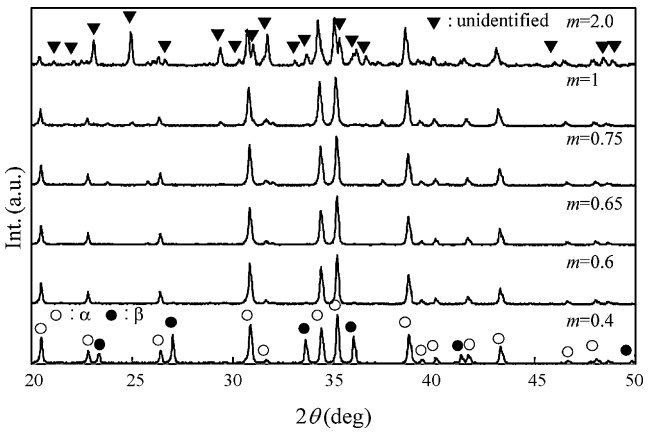

Fig. 2. X-ray powder diffraction patterns of the nominal compositions with different m values (n = 0), α: α-SiAlON, β: β-SiAlON.

The photoluminescence spectra of the powder samples were obtained by fluorescent spectrophotometer (Model F-4500, Hitachi Ltd., Japan) at room temperature with a 150 W Ushio xenon short arc lamp. The emission spectrum was corrected for the spectral response of a monochromator and Hamamatsu R928P photomultiplier tube by a light diffuser and tungsten lamp (Noma, 10 V, 4 A). The excitation spectrum was also corrected for the spectral distribution of the xenon lamp intensity using rhodamine-B as reference.

3. Results and discussion

3.1. Formation of Eu-α-SiAlON

Fig. 2 shows the XRD patterns of samples in nominal compositions with different m values (m = 0.40–2.00) and a constant n value (n = 0). As seen in Fig. 2, the single α-SiAlON phase was obtained for samples with the m value varying from 0.6 to 0.75, indicating that Eu can be dissolved completely into the α-SiAlON structure and formed limited solid solutions. When m was below 0.4, the β-phase (β-Si_3N_4 or β-SiAlON) was observed to coexist with α-SiAlON phase. While at high m values of above 0.75, the obvious unidentified phases appear gradually with increasing m. Those results suggest that the solubility limit of Eu^{2+} in oxygen-free (n = 0) α-SiAlON is less than m = 2.0 and the single phase solid solution is in the range of m = 0.6–0.75. Moreover, the shift of the diffraction peaks of Eu-α-SiAlON to low 2θ angle implies that the lattice expands with increasing m, as found in Ca-α-SiAlON:Eu^{2+} [9]. Fig. 3 presents XRD patterns of the samples with different n values (n = 0–1.0) and a constant m value (m = 0.65). As shown, the amount of β-phase increases with an increase of n. Since n stands for the oxygen content in the composition, a large n means the composition is an oxygen rich phosphor. As reported previously

Table 1
Nominal starting compositions and chemical formula of the samples.

No.	Sample name	m	n	Starting composition (wt.%)				Chemical formula
				$Eu_2Si_5N_8$	α-Si_3N_4	A1N	$A1_2O_3$	
1	m1	0.400	0	9.41	87.81	2.77	0	$Eu_{0.2}Si_{11.6}Al_{0.4}N_{16}$
2	m2	0.600	0	13.77	82.17	4.06	0	$Eu_{0.3}Si_{11.4}Al_{0.6}N_{16}$
3	m3	0.750	0	16.90	78.12	4.98	0	$Eu_{0.375}Si_{11.25}Al_{0.75}N_{16}$
4	m4	1.000	0	21.87	71.68	6.45	0	$Eu_{0.5}Si_{11}AlN_{16}$
5	m5	2.000	0	39.14	49.33	11.53	0	$EuSi_{10}Al_2N_{16}$
6	n1	0.650	0	14.83	80.80	4.37	0	$Eu_{0.325}Si_{11.35}Al_{0.65}N_{16}$
7	n2	0.650	0.065	14.83	80.30	4.51	0.36	$Eu_{0.325}Si_{11.285}Al_{0.715}O_{0.065}N_{15.9135}$
8	n3	0.650	0.130	14.83	79.79	4.66	0.72	$Eu_{0.325}Si_{11.22}Al_{0.78}O_{0.13}N_{15.87}$
9	n4	0.650	0.195	14.82	79.28	4.80	1.09	$Eu_{0.325}Si_{11.155}Al_{0.845}O_{0.195}N_{15.805}$
10	n5	0.650	0.325	14.82	78.27	5.10	1.81	$Eu_{0.325}Si_{11.025}Al_{0.975}O_{0.32}sN_{15.675}$
11	n6	0.650	0.500	14.82	76.91	5.49	2.78	$Eu_{0.325}Si_{10.85}Al_{1.15}O_{0.5}N_{15.5}$
12	n7	0.650	0.750	14.81	74.97	6.04	4.18	$Eu_{0.325}Si_{10.6}Al_{1.4}O_{0.75}N_{15.25}$
13	n8	0.650	1.000	14.81	73.03	6.60	5.57	$Eu_{0.325}Si_{10.35}Al_{1.65}ON_{15}$

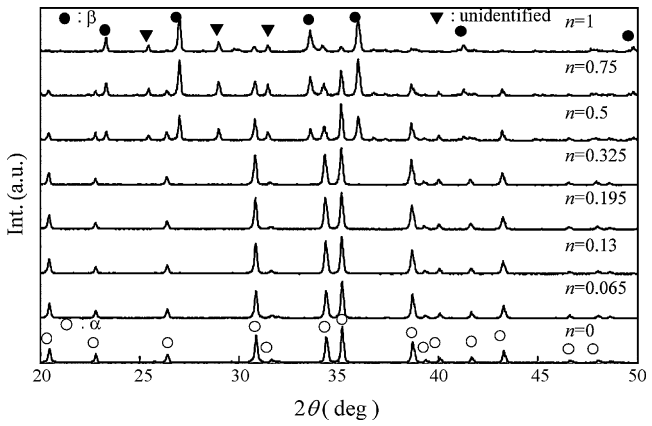

Fig. 3. X-ray powder diffraction patterns of the nominal compositions with different n values ($m = 0.65$), α: α-SiAlON, β: β-SiAlON.

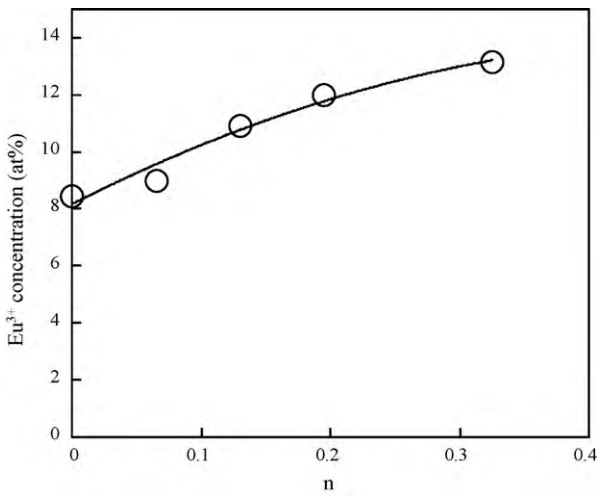

Fig. 5. Eu^{3+} concentration of the compositions with different n values ($m = 0.65$).

[23], the increment of β-phase with increasing n values can be ascribed to the excess formation of oxygen-rich liquid phase during firing, in turn promotes the formation of β-phase. Therefore, we demonstrate that Eu-α-SiAlON can be synthesized in compositions with small m and n values ($m = 0.6$–0.75 and $n = 0$–0.325). As mentioned above, Eu solely doped α-SiAlON was not available in previous studies, which indicates that the m and n values were too high to stabilize the structure of α-SiAlON by Eu^{2+} in those investigations (Shen et al. [17]: $m = 1.44$ and $n = 1.3$, Jiang et al. [18]: $m = 1.5$ and $n = 0.75$). The present result is comparable to a previous study on the formation of Sr-α-SiAlON [19]. To understand this result, the oxidation states of Eu in α-SiAlON with $m = 0.65$, $n = 0$–0.325 were estimated from XANES spectra using $Eu_2Si_5N_8$ and Eu_2O_3 spectra as references for Eu^{2+} and Eu^{3+}, respectively. Figs. 4 and 5 show that Eu-α-SiAlON is mainly composed of Eu^{2+}

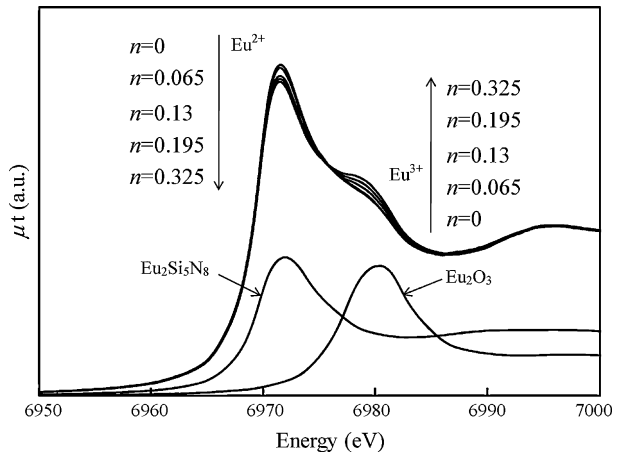

Fig. 4. Eu L_{III}-edge XANES spectra of $Eu_2Si_5N_8$, Eu_2O_3, and the nominal compositions with different n values ($m = 0.65$).

(Eu^{2+}: 87–92 at.%). The concentration of Eu^{3+} shows nearly linear increase with the increase of n, i.e., oxygen content (Fig. 5). Because the ionic size of Eu^{2+} is 1.2 Å and is similar to that of Sr^{2+} (1.21 Å) for C.N. = 7 [24], it is reasonable that the compositions of the Eu containing α-SiAlON are comparable to those of Sr-α-SiAlON. As expected, a small amount of Eu^{3+} ions is always accompanying with the Eu^{2+} ions in the Eu-compounds. The influence of the Eu^{3+} concentration on the luminescent properties will be discussed later.

3.2. Crystal structure

The X-ray powder diffraction data of Eu-α-SiAlON in nominal compositions with $m = 0.65$, $n = 0$–0.325 were used for structural refinement. The occupancy of Eu^{3+} was derived from the estimation by XAFS analysis. The ratio of Si/Al was fixed according to the composition determined by the occupancy of Eu^{2+}/Eu^{3+}. The ratio of N/O was also fixed with the nominal composition. The reliability factors, lattice parameters, and the refined structure parameters were listed in Tables 2 and 3. It can be seen that the reliability factors from the refinements are $R_{wp} = 8.35$–10.08%, $R_p = 6.42$–7.47%, and $S = 1.43$–1.72. The refined lattice parameters are increased with increasing n values from $a = 7.7829(2)$ Å to $a = 7.7938(2)$ Å, and from $c = 5.64709(5)$ Å to $c = 5.65974(5)$ Å (Fig. 6). These values are slightly smaller than that of Sr-α-SiAlON ($a = 7.79189(5)$ Å, $c = 5.65377(2)$ Å) [19] in agreement with the fact that Eu^{2+} is smaller than that of Sr^{2+} [24]. Additionally, the lattice parameters of the sample with $n = 0$ in starting composition are slightly shorter than that of Sr-α-SiAlON. It can be ascribed to the difference of m value in the starting composition between Eu- and Sr-α-SiAlONs ($m = 0.65$ for Eu-α-SiAlON, and $m = 0.75$ for Sr-α-SiAlON). The increment of the lattice parameters shown in Table 2 is attributable to the increased n values since the average Si–N bond length of 1.74 Å is shorter than

Table 2
Crystallographic data for Eu-α-SiAlON.

	n1	n2	n3	n4	n5
Crystal system			Trigonal		
Space group			*P*31*c* (no. 159)		
Z			1		
a (Å)	7.7829(2)	7.7850(2)	7.7885(2)	7.7907(2)	7.7938(2)
c (Å)	5.64709(5)	5.64928(6)	5.65264(5)	5.65527(5)	5.65974(5)
V (Å^3)	296.24(1)	296.51(1)	296.95(1)	297.26(1)	297.74(1)
R_{wp}	9.15	10.08	8.35	8.69	9.64
R_p	6.86	7.47	6.42	6.76	7.44
S	1.62	1.72	1.43	1.47	1.62

Table 3
The refined atomic coordinates, occupancies, and isotropic atomic displacement parameters for Eu-α-SiAlON.

Atom	Wykoff position	Occ	*x*	*y*	*z*	*B* (Å^2)
n1 (*n* = 0)						
Eu^{2+}/Eu^{3+}	2b	0.1091(6)/0.0101	1/3	2/3	0.244(2)	0.71
Si/Al1	6c	0.9586/0.0414	0.5107(2)	0.0818(2)	0.219(2)	0.47
Si/A12	6c	0.9586/0.0414	0.1692(2)	0.2539(2)	0.013(2)	0.58
N/O1	2a	1/0	0	0	0	0.16
N/O2	2b	1/0	1/3	2/3	0.658(2)	0.16
N/O3	6c	1/0	0.3494(4)	−0.0401(5)	0.009(2)	0.16
N/O4	6c	1/0	0.3186(4)	0.3112(4)	0.271(2)	0.16
n2 (*n* = 0.065)						
Eu^{2+}/Eu^{3+}	2b	0.1137(7)/0.0112	1/3	2/3	0.242(2)	0.71
Si/Al1	6c	0.9511/0.0489	0.5103(2)	0.0819(2)	0.217(2)	0.47
Si/Al2	6c	0.9511/0.0489	0.1695(2)	0.2542(2)	0.010(2)	0.58
N/O1	2a	0.9959/0.0041	0	0	0	0.16
N/O2	2b	0.9959/0.0041	1/3	2/3	0.658(2)	0.16
N/O3	6c	0.9959/0.0041	0.3495(4)	−0.0385(5)	0.008(2)	0.16
N/O4	6c	0.9959/0.0041	0.3183(4)	0.3111(5)	0.267(2)	0.16
n3 (*n* = 0.13)						
Eu^{2+}/Eu^{3+}	2b	0.1236(6)/0.0152	1/3	2/3	0.241(2)	0.71
Si/Al1	6c	0.9404/0.0596	0.5110(2)	0.0820(2)	0.219(1)	0.47
Si/Al2	6c	0.9404/0.0596	0.1695(2)	0.2541(1)	0.012(2)	0.58
N/O1	2a	0.9919/0.0081	0	0	0	0.16
N/O2	2b	0.9919/0.0081	1/3	2/3	0.664(2)	0.16
N/O3	6c	0.9919/0.0081	0.3482(3)	−0.0394(4)	0.009(2)	0.16
N/O4	6c	0.9919/0.0081	0.3190(4)	0.3107(4)	0.272(2)	0.16
n4 (*n* = 0.195)						
Eu^{2+}/Eu^{3+}	2b	0.1298(6)/0.0177	1/3	2/3	0.240(2)	0.71
Si/Al1	6c	0.9316/0.0684	0.5108(2)	0.0815(2)	0.219(2)	0.47
Si/Al2	6c	0.9316/0.0684	0.1700(2)	0.2542(2)	0.011(2)	0.58
N/O1	2a	0.9878/0.0122	0	0	0	0.16
N/O2	2b	0.9878/0.0122	1/3	2/3	0.662(2)	0.16
N/O3	6c	0.9878/0.0122	0.3484(3)	−0.0387(4)	0.005(2)	0.16
N/O4	6c	0.9878/0.0122	0.3187(4)	0.3109(4)	0.274(2)	0.16
n5 (*n* = 0.325)						
Eu^{2+}/Eu^{3+}	2b	0.1365(6)/0.0206	1/3	2/3	0.246(2)	0.71
Si/Al1	6c	0.9171/0.0829	0.5106(2)	0.0813(2)	0.224(2)	0.47
Si/Al2	6c	0.9171/0.0829	0.1698(2)	0.2539(2)	0.017(2)	0.58
N/O1	2a	0.9797/0.0203	0	0	0	0.16
N/O2	2b	0.9797/0.0203	1/3	2/3	0.668(2)	0.16
N/O3	6c	0.9797/0.0203	0.3480(4)	−0.0387(5)	0.012(2)	0.16
N/O4	6c	0.9797/0.0203	0.3186(4)	0.3101(5)	0.280(2)	0.16

that of Al–N (1.87 Å) and Al–O (1.75 Å). As reported previously, the lattice parameters can be related to *m* and *n* by using the following equations [25]:

$$\Delta a\ (\text{Å}) = 0.045m + 0.009n \quad (2)$$

$$\Delta c\,(\text{Å}) = 0.04m + 0.008n \quad (3)$$

The projection of the crystal structure of Eu-α-SiAlON is shown in Fig. 7(a). Similar to other metal α-SiAlON, the Eu-α-SiAlON structure has the expanded α-Si_3N_4 structure built up by the three-dimensional (Si, Al)–(N, O) network [16]. The α-SiAlON structure is stabilized by the introduction of Eu in the sevenfold coordination sites. The local structure of the Eu site in the α-SiAlON structure is shown in Fig. 7(b) and the corresponding bonding distances of Eu–N/O are listed in Table 4. The average bond lengths of the first nearest Eu–N/O bonds range from 2.607 to 2.6268 Å. These values also agree well with the previously reported average bond length of Sr–N/O (2.618 Å). The increment of the average bond length with increasing *n* value is readily ascribed to the enlargement of (Si, Al)–(O, N) network as mentioned above.

Table 4
Selected bonding distances (in Å) in the local structure of the Eu site.

	Distance (Å)				
	n1	n2	n3	n4	n5
Eu^{iv}–$N/O2^{iv}$	2.333(15)	2.35(2)	2.388(13)	2.387(13)	2.39(2)
Eu^{iv}–$N/O3^{vi}$	2.590(9)	2.598(9)	2.591(8)	2.604(8)	2.604(9)
Eu^{v}–$N/O3^{V}$	2.590(9)	2.598(9)	2.591(8)	2.604(8)	2.604(9)
Eu^{iv}–$N/O3^{iv}$	2.590(9)	2.598(9)	2.591(8)	2.604(8)	2.604(9)
Eu^{iv}–$N/O4^{v}$	2.715(2)	2.716(2)	2.724(2)	2.723(2)	2.730(3)
Eu^{iv}–$N/O4^{vi}$	2.715(2)	2.716(2)	2.724(2)	2.723(2)	2.730(2)
Eu^{iv}–$N/O4^{iv}$	2.715(3)	2.716(4)	2.724(3)	2.723(3)	2.730(4)
Average	2.607	2.6132	2.6189	2.6242	2.6268

Symmetry operations are (i) *x*, *y*, *z*; (ii) −*y*, *x* − *y*, *z*; (iii) −*x* + *y*, −*x*, *z*; (iv) *y*, *x*, *z* + 1/2; (v) *x* − *y*, −*y*, *z* + 1/2; (vi) −*x*, −*x* + *y*, *z* + 1/2.

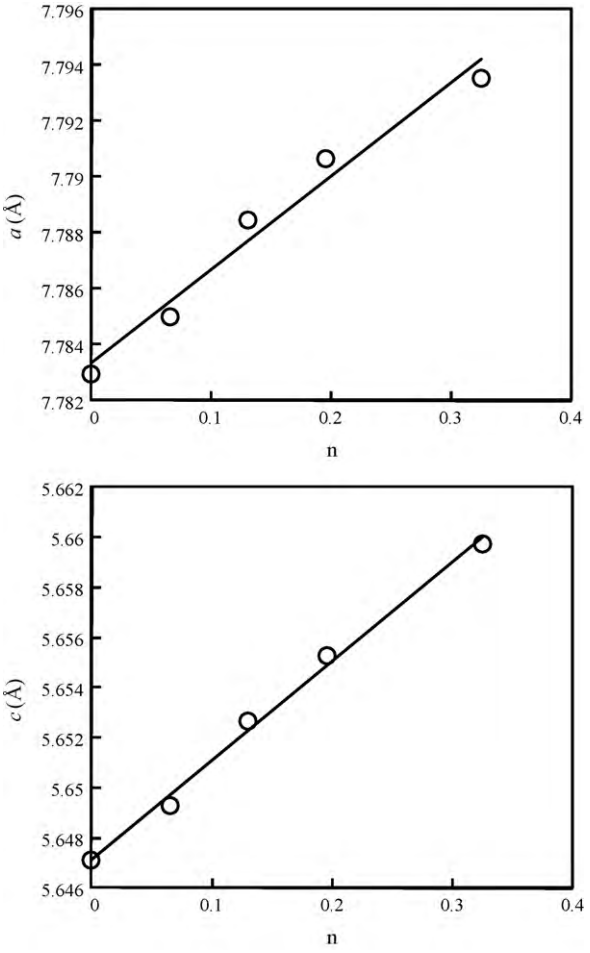

Fig. 6. Lattice parameters of Eu-α-SiAlON as a function of the nominal compositions with different n values ($m = 0.65$).

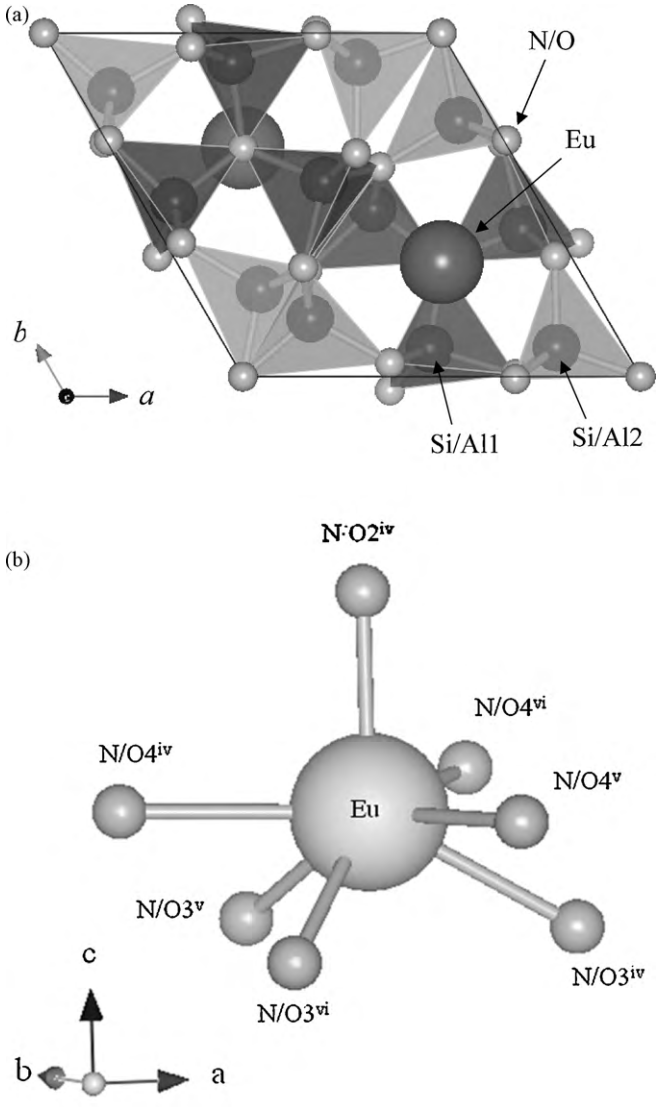

Fig. 7. (a) Crystal structures of Eu-α-SiAlON projected along the [0 0 1] direction. (b) The local structure of the Eu site in the α-SiAlON structure.

3.3. Photoluminescence properties

Fig. 8 shows the excitation and emission spectra of Eu-α-SiAlON. The excitation spectra of Eu-α-SiAlON are in the optical spectral region from the UV to visible part. Approximately, three broad bands are observed in the excitation spectrum with the maxima at about 300 nm, 400 nm, and 440 nm corresponding to $4f^7 \rightarrow 4f^6 5d$ transition of Eu^{2+}. The emission spectrum exhibits a single broad emission band ranging from 470 nm to 730 nm peaking at about 590 nm. This emission band is attributable to the allowed $4f^6 5d \rightarrow 4f^7$ transition of Eu^{2+}. Compared with Sr-α-SiAlON:Eu^{2+} ($\lambda_{em} = 585$ nm) [19], the red-shift of emission band of Eu-α-SiAlON is expected because of the energy transfer between Eu^{2+} ions and/or re-absorption of Eu^{2+} at higher Eu concentration [15]. The characteristic luminescence of Eu^{3+} with sharp lines between 560 nm and 630 nm is hardly observed, which is ascribed to the small Eu^{3+}/Eu^{2+} ratio, as expected in the nitrogen-rich environment. The emission intensity of Eu-α-SiAlON significantly decreased with increasing n value which is strongly related to the oxygen content in Eu-α-SiAlON, as a result of the markedly increased Eu^{3+} concentration. As a luminescent killer, high concentration of Eu^{3+} can significantly reduce the emission intensity of Eu^{2+}. It suggests that the luminescent intensity of Eu^{2+} activated nitride phosphors containing Eu^{3+} could be further improved by the decrease of Eu^{3+} concentration if the impurity oxygen can be controllable in the hosts.

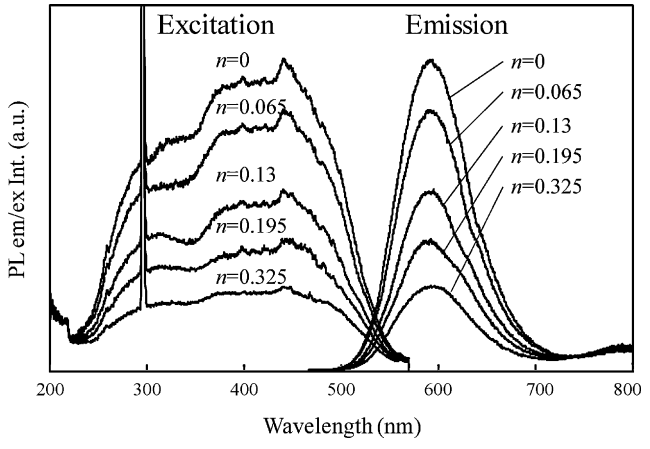

Fig. 8. Excitation and emission spectra of the Eu-α-SiAlON samples with different n values ($m = 0.65$) ($\lambda_{exc} = 440$ nm, $\lambda_{em} = 590$ nm).

4. Conclusions

Eu-α-SiAlON was successfully synthesized by gas-pressure sintering at 1900 °C for 6 h under 1 MPa nitrogen atmosphere. High purity Eu-α-SiAlON phase was obtained in nominal compositions with small m and n values (m = 0.6–0.75 and n = 0–0.325). The XANES spectrum revealed that Eu ion in Eu-α-SiAlON was mainly in divalent state with a small amount of Eu in the trivalent state. The Rietveld refinements showed that the lattice parameters of Eu-α-SiAlON were comparable to those of Sr-α-SiAlON. The lattice parameters of the samples with m = 0.65, n = 0–0.325 increased with increasing n values. Eu-α-SiAlON exhibited yellow emission with a peak wavelength of 590 nm under the blue excitation. The emission intensity decreased significantly with increasing the Eu^{3+} concentration. It suggests that the luminescent intensity of Eu^{2+} activated oxynitride phosphors can be enhanced by the decrease of the Eu^{3+} concentration.

Acknowledgements

The synchrotron radiation experiments were performed at the BL14B2 in the SPring-8 with the approval of the Japan Synchrotron Radiation Research Institute (JASRI) (Proposal No. 2009B2079). Authors greatly thank for the technical support and discussions from JASRI.

References

[1] H.A. Hoppe, H. Lutz, P. Morys, W. Schnick, A. Seilmeier, J. Phys. Chem. Solids 61 (2000) 2001.
[2] Y.Q. Li, J.E.J. van Steen, J.W.H. van Krevel, G. Botty, A.C.A. Delsing, F.J. DiSalvo, G. de With, H.T. Hintzen, J. Alloys Compd. 417 (2006) 273.
[3] K. Uheda, N. Hirosaki, Y. Yamamoto, A. Naito, T. Nakajima, H. Yamamoto, Electrochem. Solid State Lett. 9 (2006) H22.
[4] K. Uheda, N. Hirosaki, H. Yamamoto, Phys. Status Solidi A203 (2006) 2712.
[5] H. Watanabe, N. Kijima, J. Alloys Compd. 475 (2009) 434.
[6] C. Hecht, F. Stadler, P.J. Schmidt, J.S. auf der Günne, V. Baumann, W. Schnick, Chem. Mater. 21 (2009) 1595.
[7] J.W.H. van Krevel, J.W.T. van Rutten, H. Mandal, H.T. Hintzen, R. Metselaar, J. Solid State Chem. 165 (2002) 19.
[8] R.-J. Xie, M. Mitomo, K. Uheda, F.-F. Xu, Y. Akimune, J. Am. Ceram. Soc. 85 (2002) 1229.
[9] R.-J. Xie, N. Hirosaki, K. Sakuma, Y. Yamamoto, M. Mitomo, Appl. Phys. Lett. 84 (2004) 5404.
[10] R.-J. Xie, N. Hirosaki, M. Mitomo, Y. Yamamoto, T. Suehiro, K. Sakuma, J. Phys. Chem. B 108 (2004) 12027.
[11] N. Hirosaki, R.-J. Xie, K. Kimoto, T. Sekiguchi, Y. Yamamoto, T. Suehiro, M. Mitomo, Appl. Phys. Lett. 86 (2005) 211905.
[12] Y. Fukuda, K. Ishida, I. Mitsuishi, S. Nunoue, Appl. Phys. Express 2 (2009), 012401–3.
[13] O. Oeckler, J.A. Kechele, H. Koss, P.J. Schmidt, W. Schnick, Chem. Eur. J. 15 (2009) 5311.
[14] J.W.H. van Krevel, H.T. Hintzen, R. Metselaar, A. Meijerink, J. Alloys Compd. 268 (1998) 272.
[15] K. Sakuma, N. Hirosaki, R.-J. Xie, J. Lumin. 126 (2007) 843.
[16] G.Z. Cao, R. Metselaar, Chem. Mater. 3 (1991) 242.
[17] Z. Shen, M. Nygren, P. Wang, J. Feng, J. Mater. Sci. Lett. 17 (1998) 1703.
[18] J.-X. Jiang, P.-L. Wang, W.-B. He, W.-W. Chen, H.-R. Zhuang, Y.-B. Cheng, D.-S. Yan, Mater. Lett. 59 (2005) 205.
[19] K. Shioi, N. Hirosaki, R.-J. Xie, T. Takeda, Y.Q. Li, Y. Matsushita, J. Am. Ceram. Soc. 93 (2010) 465.
[20] X. Piao, T. Horikawa, H. Hanzawa, K. Machida, Appl. Phys. Lett. 88 (2006) 161908.
[21] F. Izumi, K. Momma, Solid State Phenom. 130 (2007) 15.
[22] Momma, K. Izumi, J. Appl. Crystallogr. 41 (2008) 653.
[23] H.L. Li, R.-J. Xie, N. Hirosaki, T. Suehiro, Y. Yajima, J. Electrochem. Soc. 155 (2008) J175.
[24] R.D. Shannon, Acta Crystollgr. A32 (1976) 751.
[25] S. Hampshire, H.K. Park, D.P. Thompson, K.H. Jack, Nature (Lond.) 274 (1978) 880.